Power Control in D2D-Based Multi-Antenna V2V Underlay Cellular Networks with Rate Constraints

Xinxin Liu, Yunzhou Li, Limin Xiao, and Jing Wang
Tsinghua National Laboratory for Information Science and Technology
Department of Electronic Engineering, Tsinghua University, Beijing, China

Abstract—**Device-to-device (D2D) communication has been proposed as a solution for vehicle-to-vehicle (V2V) communication, which has strict requirements on reliability and latency. Previous works on V2V communication typically assume single-antenna users, which ignore the potential of multiple antennas. By contrast, this paper studies an uplink power control problem in multi-antenna V2V underlay cellular networks. We first derive the lower bounds on ergodic rates of multi-antenna V2V users and cellular users for maximum-ratio combining and zero-forcing detection. Using these rate lower bounds, we formulate a large-scale fading based power control problem to maximize the sum rate of cellular users while introducing the rate constraints of V2V users. Moreover, the geometric programming technique is adopted to solve the optimization power control problem. Simulation results show that the proposed rate-constrained power control scheme provides more reliable V2V communications with higher data rates at the price of a small loss of network sum rate, compared to the fixed maximum power scheme.**

I. Introduction

With the increasing demand for vehicular communications, vehicle-to-vehicle (V2V) communication has received a lot of attention in recent years. V2V has the potential to enhance road safety, improve traffic efficiency, provide location-based services, and realize autonomous driving, while requiring high reliability, low latency, and high data rates [1].

Device-to-device (D2D) communication enables proximity devices to transmit signals directly without routing by a base station (BS). It has been identified as a key component for future 5G cellular networks [2]. Besides, the D2D underlay cellular network can support V2V communication by means of D2D-based communication, due to three promising gains (i.e., proximity gain, reuse gain, and hop gain) [3]. However, in D2D-based V2V underlay cellular networks, where the cellular radio resources are reused by V2V user equipments (UEs), mutual interference may be serious if not designed properly. Moreover, how to guarantee the reliability and data rates of V2V communications is still a challenge. Thus, interference management and resource allocation become key design aspects in V2V underlay cellular networks.

This work was supported by Science Fund for Creative Research Groups of NSFC (61321061), National Nature Science Foundation of China (61631013), National Basic Research Program of China (2013CB329002), China's 863 Project (2015AA01A706), National Major Project (2016ZX03001023-003), Program for New Century Excellent Talents in University (NCET-13-0321), Tsinghua University Initiative Scientific Research Program (2011THZ02-2), and Tsinghua-Qualcomm Joint Research Program.

In [4], a heuristic location-dependent resource allocation method was proposed for D2D-based V2V communications. The authors in [5] proposed a separate resource allocation and power control scheme for single-cell V2V underlay cellular networks. However, all the UEs and the BS are equipped with only one antenna in these works, which ignore the potential of multiple antennas.

In this paper, we consider a single-cell V2V underlay cellular network with uplink spectrum sharing, where the BS and UEs are equipped with multiple antennas. [1] With perfect channel state information (CSI) of desired V2V channels, [2]we first derive the lower bounds on ergodic rates of V2V transmitters for maximum-ratio combining (MRC) and zero-forcing (ZF) detection. Then we derive the lower bounds on ergodic rates of cellular UEs, assuming that perfect CSI from cellular UEs and V2V transmitters is known at the BS. Using these rate lower bounds, a power control problem is formulated to meet the rate requirements of V2V UEs and maximize the sum rate of cellular UEs. Further, the geometric programming (GP) technique is adopted to solve the optimization problem. Simulation results verify that the analytical lower bounds are accurate. The results also show that the proposed power control scheme provides more reliable V2V communications with higher data rates while the sum rate of cellular and V2V UEs is slightly degraded, compared to the fixed maximum power scheme.

Note that power control problems have been discussed in D2D underlay cellular networks. The authors in [6] derived the optimal power control to maximize the sum rate in a restricted scenario with one single-antenna cellular UE and one pair of single-antenna D2D UEs. In [7], a power control problem was studied to maximize the sum rate with signal-to-interference-plus-noise ratio (SINR) constraints of single-antenna UEs. However, existing works [6], [7] assume that the BS know the CSI of all the involved links. In practice, reporting instantaneous CSI of D2D (V2V) links to the BS will lead to large overhead. In contrast, our work avoids reporting CSI and studies a large-scale fading based power control problem in multi-antenna V2V underlay cellular networks.

[1]We focus on the intra-cell mutual interference in a single-cell scenario since the results are clearly and easily comprehensible. The extension to the multi-cell scenario is left for future work.

[2]Note that the CSI of interfering channels from other V2V transmitters and cellular UEs is not known.

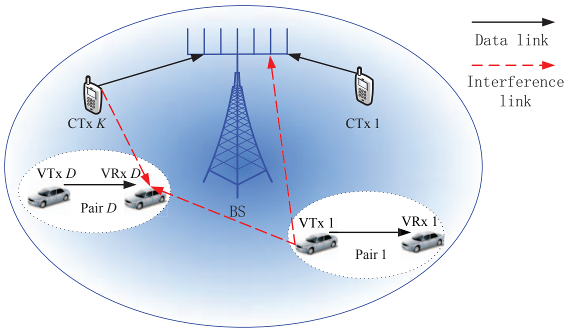

Fig. 1. An uplink D2D-based V2V underlay cellular network.

II. System Model

We consider a single-cell uplink D2D-based V2V underlay cellular network shown in Fig. 1, where the BS is equipped with M antennas and serves K cellular UEs simultaneously. To generalize the system model, D pairs D2D-based V2V UEs and K cellular UEs use the same time-frequency resources, leading to mutual interference. Each V2V pair consists of a transmitter and a receiver. For delay-sensitive V2V communications, exploiting time diversity may not be possible. In this case, antenna diversity (or spatial diversity), which can be obtained by placing multiple antennas at the transmitter and the receiver, is promising to improve network performance [8]. Hence, we consider that cellular UEs and V2V UEs are equipped with N_c and N_d antennas, respectively.

We focus on MIMO transmissions in this paper, i.e., cellular UEs transmit N_c streams and V2V transmitters transmit N streams, while the BS and V2V receivers respectively use M and N_d antennas to receive signals. In the following, we use $\mathcal{C} = \{1, 2, \dots, K\}$ and $\mathcal{V} = \{1, 2, \dots, D\}$ to denote the sets of cellular UEs and V2V pairs, respectively.

The $N_d \times 1$ dimensional baseband received signal at the receiver of V2V pair i is given by

$$\mathbf{y}_i^{\mathrm{v}} = \sum_{j\in\mathcal{V}} \mathbf{H}_{ji}^{\mathrm{vv}} \mathbf{W}_j^{\mathrm{v}} (\mathbf{P}_j^{\mathrm{v}})^{\frac{1}{2}} \mathbf{s}_j^{\mathrm{v}} + \sum_{k\in\mathcal{C}} \mathbf{H}_{ki}^{\mathrm{cv}} (\mathbf{P}_k^{\mathrm{c}})^{\frac{1}{2}} \mathbf{s}_k^{\mathrm{c}} + \mathbf{n}_i^{\mathrm{v}} \quad (1)$$

where $\mathbf{H}_{ji}^{\mathrm{vv}}$=$[\mathbf{h}_{ji1}^{\mathrm{vv}}, \cdots, \mathbf{h}_{jiN_d}^{\mathrm{vv}}] \in \mathbb{C}^{N_d \times N_d}$ is the channel matrix from V2V transmitter j to V2V receiver i, $\mathbf{W}_j^{\mathrm{v}} \in \mathbb{C}^{N_d \times N}$ is the precoding matrix used by V2V transmitter j, $\mathbf{P}_j^{\mathrm{v}} = \mathrm{diag}\{p_{j1}^{\mathrm{v}}, \cdots, p_{jN}^{\mathrm{v}}\}$ with $\mathrm{tr}\{(\mathbf{P}_j^{\mathrm{v}})^{\frac{1}{2}} (\mathbf{W}_j^{\mathrm{v}})^H \mathbf{W}_j^{\mathrm{v}} (\mathbf{P}_j^{\mathrm{v}})^{\frac{1}{2}}\} = P_j^{\mathrm{v}}$ is the power allocation matrix of V2V transmitter j, $\mathbf{s}_j^{\mathrm{v}} = [s_{j1}^{\mathrm{v}}, \cdots, s_{jN}^{\mathrm{v}}]^T \sim \mathcal{CN}(0, \mathbf{I}_N)$ is the data symbol vector of V2V transmitter j, $\mathbf{H}_{ki}^{\mathrm{cv}} \in \mathbb{C}^{N_d \times N_c}$, $\mathbf{P}_k^{\mathrm{c}} = \mathrm{diag}\{p_{k1}^{\mathrm{c}}, \cdots, p_{kN_c}^{\mathrm{c}}\}$ with $\mathrm{tr}\{\mathbf{P}_k^{\mathrm{c}}\} = P_k^{\mathrm{c}}$, and $\mathbf{s}_k^{\mathrm{c}} \in \mathbb{C}^{N_c \times 1}$ are similarly defined for cellular UE k, and $\mathbf{n}_i^{\mathrm{v}} \sim \mathcal{CN}(0, \sigma^2 \mathbf{I}_{N_d})$ is the noise vector at V2V receiver i. Similarly, the $M \times 1$ dimensional baseband received signal at the BS is given by

$$\mathbf{y}^{\mathrm{c}} = \sum_{k\in\mathcal{C}} \mathbf{H}_k^{\mathrm{c}} \left(\mathbf{P}_k^{\mathrm{c}}\right)^{\frac{1}{2}} \mathbf{s}_k^{\mathrm{c}} + \sum_{j\in\mathcal{V}} \mathbf{H}_j^{\mathrm{v}} \mathbf{W}_j^{\mathrm{v}} \left(\mathbf{P}_j^{\mathrm{v}}\right)^{\frac{1}{2}} \mathbf{s}_j^{\mathrm{v}} + \mathbf{n}^{\mathrm{c}} \quad (2)$$

where $\mathbf{H}_k^{\mathrm{c}} = [\mathbf{h}_{k1}^{\mathrm{c}}, \cdots, \mathbf{h}_{kN_c}^{\mathrm{c}}] \in \mathbb{C}^{M \times N_c}$ is the channel matrix from cellular UE k to the BS, $\mathbf{H}_j^{\mathrm{v}} \in \mathbb{C}^{M \times N_d}$ is the channel matrix from V2V transmitter j to the BS, and $\mathbf{n}^{\mathrm{c}} \sim \mathcal{CN}(0, \sigma^2 \mathbf{I}_M)$ is the noise vector at the BS.

If the antennas are separated by at least a few wavelengths, then all channels between different antenna pairs are mutually independent (see [Chapter 3.3, 8] for details). It is reasonable to place multiple antennas far apart at a vehicular UE since it has a big size. Thus, we assume that all channel vectors are mutually independent. The channel vectors from different UEs to V2V receiver i and the BS, which follow zero-mean circularly symmetric complex Gaussian distribution, are respectively defined as

$$\mathbf{h}_{jil}^{\mathrm{xv}} \sim \mathcal{CN}(0, \beta_{jil}^{\mathrm{xv}} \mathbf{I}_{N_d}) \quad (3)$$

$$\mathbf{h}_{kl}^{\mathrm{y}} \sim \mathcal{CN}(0, \beta_{kl}^{\mathrm{y}} \mathbf{I}_M) \quad (4)$$

where the superscript "xv" denotes "vv" (referred to as V2V transmitter to V2V receiver) or "cv" (cellular UE to V2V receiver), $\beta_{jil}^{\mathrm{xv}}$ is the large-scale fading coefficient from the lth antenna of UE j to V2V receiver i, the superscript "y" denotes "c" (cellular UE) or "v" (V2V transmitter), β_{kl}^{y} is the large-scale fading coefficient from the the lth antenna of UE k to the BS.

III. Uplink Rate Analysis

To avoid the high complexity of non-linear receivers (e.g., maximum-likelihood), we consider linear processing receivers such as MRC and ZF. In this section, we analyze the uplink rates of multi-antenna V2V UEs and cellular UEs for MRC and ZF detection. [3]

A. V2V Rate

Based on the received signal $\mathbf{y}_i^{\mathrm{v}}$ in (1), $\mathbf{H}_{ji}^{\mathrm{evv}} = \mathbf{H}_{ji}^{\mathrm{vv}} \mathbf{W}_j^{\mathrm{v}}$ is defined as the effective channel from V2V transmitter j to V2V receiver i. Assuming that perfect CSI of the desired V2V channel is known at V2V receiver i, we consider two linear detectors MRC and ZF, i.e.,

$$\mathbf{A}_i^{\mathrm{v}} = \begin{cases} \mathbf{H}_{ii}^{\mathrm{evv}} & \text{for MRC} \\ \bar{\mathbf{H}}_{ii}^{\mathrm{evv}} \left((\bar{\mathbf{H}}_{ii}^{\mathrm{evv}})^H \bar{\mathbf{H}}_{ii}^{\mathrm{evv}} \right)^{-1} & \text{for ZF} \end{cases} \quad (5)$$

where $\bar{\mathbf{H}}_{ii}^{\mathrm{evv}} = \mathbf{H}_{ii}^{\mathrm{evv}} (\mathbf{P}_i^{\mathrm{v}})^{\frac{1}{2}}$. Let $\mathbf{a}_{im}^{\mathrm{v}} \in \mathbb{C}^{N_d \times 1}$ be the mth column of the matrix $\mathbf{A}_i^{\mathrm{v}}$. Using the detector $\mathbf{a}_{im}^{\mathrm{v}}$ corresponding to the mth stream of V2V transmitter i, V2V receiver i obtains the post-processing received signal, given as

$$\begin{aligned} \tilde{y}_{im}^{\mathrm{v}} = (\mathbf{a}_{im}^{\mathrm{v}})^H \mathbf{y}_i^{\mathrm{v}} = (\mathbf{a}_{im}^{\mathrm{v}})^H \sum_{j\in\mathcal{V}} \mathbf{H}_{ji}^{\mathrm{evv}} (\mathbf{P}_j^{\mathrm{v}})^{\frac{1}{2}} \mathbf{s}_j^{\mathrm{v}} \\ + (\mathbf{a}_{im}^{\mathrm{v}})^H \sum_{k\in\mathcal{C}} \mathbf{H}_{ki}^{\mathrm{cv}} (\mathbf{P}_k^{\mathrm{c}})^{\frac{1}{2}} \mathbf{s}_k^{\mathrm{c}} + (\mathbf{a}_{im}^{\mathrm{v}})^H \mathbf{n}_i^{\mathrm{v}}. \end{aligned} \quad (6)$$

Thus, the post-processing SINR corresponding to the mth stream of V2V transmitter i can be given as

$$\gamma_{im}^{\mathrm{v}} = \frac{p_{im}^{\mathrm{v}} \left| (\mathbf{a}_{im}^{\mathrm{v}})^H \mathbf{h}_{iim}^{\mathrm{evv}} \right|^2}{\sum\limits_{k\neq m} p_{ik}^{\mathrm{v}} \left| (\mathbf{a}_{im}^{\mathrm{v}})^H \mathbf{h}_{iik}^{\mathrm{evv}} \right|^2 + (\mathbf{a}_{im}^{\mathrm{v}})^H \mathbf{Z}_i^{\mathrm{v}} \mathbf{a}_{im}^{\mathrm{v}} + \sigma^2 \|\mathbf{a}_{im}^{\mathrm{v}}\|^2} \quad (7)$$

[3]The ZF detector is selected to amplify the desired signal and suppress interference from other streams or UEs in the spatial domain.

$$\gamma_{km}^{\mathrm{c}} = \frac{p_{km}^{\mathrm{c}} \left|(\mathbf{a}_{km}^{\mathrm{c}})^H \mathbf{h}_{km}^{\mathrm{c}}\right|^2}{\mathbb{E}\left[(\mathbf{a}_{km}^{\mathrm{c}})^H \left(\sum_{q\neq m} p_{kq}^{\mathrm{c}} \mathbf{h}_{kq}^{\mathrm{c}} (\mathbf{h}_{kq}^{\mathrm{c}})^H + \sum_{i\neq k} \mathbf{H}_i^{\mathrm{c}} \mathbf{P}_i^{\mathrm{c}} (\mathbf{H}_i^{\mathrm{c}})^H + \sum_{j\in\mathcal{V}} \mathbf{H}_j^{\mathrm{ev}} \mathbf{P}_j^{\mathrm{v}} (\mathbf{H}_j^{\mathrm{ev}})^H + \sigma^2 \mathbf{I}_M\right) \mathbf{a}_{km}^{\mathrm{c}}\right]}. \quad (12)$$

where $\mathbf{Z}_i^{\mathrm{v}}$ is the interference covariance matrix of other V2V transmitters and cellular UEs, i.e.,

$$\mathbf{Z}_i^{\mathrm{v}} = \mathbb{E}\Big[\sum_{j\neq i} \mathbf{H}_{ji}^{\mathrm{evv}} \mathbf{P}_j^{\mathrm{v}} (\mathbf{H}_{ji}^{\mathrm{evv}})^H + \sum_{k\in\mathcal{C}} \mathbf{H}_{ki}^{\mathrm{cv}} \mathbf{P}_k^{\mathrm{c}} (\mathbf{H}_{ki}^{\mathrm{cv}})^H\Big]. \quad (8)$$

Using a bound based on the worst-case Gaussian noise [9], the ergodic rate of V2V transmitter i can be given as

$$R_i^{\mathrm{v}} = \mathbb{E}\Big[\sum_{m=1}^{N} \log_2\left(1+\gamma_{im}^{\mathrm{v}}\right)\Big]. \quad (9)$$

B. Cellular Rate

Based on the received signal $\mathbf{y}^{\mathrm{c}}$ in (2), $\mathbf{H}_j^{\mathrm{ev}} = \mathbf{H}_j^{\mathrm{v}} \mathbf{W}_j^{\mathrm{v}}$ is defined as the effective channel from V2V transmitter j to the BS. With perfect CSI from not only cellular UEs but also V2V transmitters to the BS, we consider two linear detectors MRC and interference-aware ZF at the BS, i.e.,

$$\mathbf{A}^{\mathrm{c}} = \begin{cases} \mathbf{H}^{\mathrm{c}} & \text{for MRC} \\ \bar{\mathbf{H}}\left(\bar{\mathbf{H}}^H \bar{\mathbf{H}}\right)^{-1} & \text{for interference-aware ZF} \end{cases} \quad (10)$$

where $\mathbf{H}^{\mathrm{c}} = [\mathbf{H}_1^{\mathrm{c}}, \mathbf{H}_2^{\mathrm{c}}, \cdots, \mathbf{H}_K^{\mathrm{c}}]$ denotes the CSI from all the cellular UEs, $\bar{\mathbf{H}} = \mathbf{H}(\mathbf{P}_{\mathrm{b}})^{\frac{1}{2}}$, $\mathbf{H} = [\mathbf{H}^{\mathrm{c}}, \mathbf{H}_1^{\mathrm{ev}}, \mathbf{H}_2^{\mathrm{ev}}, \cdots, \mathbf{H}_D^{\mathrm{ev}}]$ denotes the CSI from cellular UEs and V2V transmitters, and $\mathbf{P}_{\mathrm{b}} = \mathrm{diag}\{\mathbf{P}_1^{\mathrm{c}}, \cdots, \mathbf{P}_K^{\mathrm{c}}, \mathbf{P}_1^{\mathrm{v}}, \cdots, \mathbf{P}_D^{\mathrm{v}}\} \in \mathbb{C}^{B\times B}$ with $B = KN_c + DN$. Let $\mathbf{a}_{km}^{\mathrm{c}} \in \mathbb{C}^{M\times 1}$ denote the fth column of the matrix $\mathbf{A}^{\mathrm{c}}$ where $f = (k-1)N_c + m$. Using the detector $\mathbf{a}_{km}^{\mathrm{c}}$ corresponding to the mth stream of cellular UE k, the BS obtains the post-processing received signal, given as

$$\begin{aligned}\tilde{y}_{km}^{\mathrm{c}} &= (\mathbf{a}_{km}^{\mathrm{c}})^H \mathbf{y}^{\mathrm{c}} = (\mathbf{a}_{km}^{\mathrm{c}})^H \sum_{k\in\mathcal{C}} \mathbf{H}_k^{\mathrm{c}} \left(\mathbf{P}_k^{\mathrm{c}}\right)^{\frac{1}{2}} \mathbf{s}_k^{\mathrm{c}} \\ &+ (\mathbf{a}_{km}^{\mathrm{c}})^H \sum_{j\in\mathcal{V}} \mathbf{H}_j^{\mathrm{ev}} \left(\mathbf{P}_j^{\mathrm{v}}\right)^{\frac{1}{2}} \mathbf{s}_j^{\mathrm{v}} + (\mathbf{a}_{km}^{\mathrm{c}})^H \mathbf{n}^{\mathrm{c}}. \end{aligned} \quad (11)$$

In this case, the SINR corresponding to the mth stream of cellular UE k is shown in (12) at the top of this page. Then the ergodic rate of cellular UE k can be given as

$$R_k^{\mathrm{c}} = \mathbb{E}\Big[\sum_{m=1}^{N_c} \log_2\left(1+\gamma_{km}^{\mathrm{c}}\right)\Big]. \quad (13)$$

IV. Lower Bounds on Ergodic Rates

In this section, we derive the lower bounds on ergodic rates of multi-antenna V2V UEs and cellular UEs for MRC and ZF detection to provide more insights. In the following, it is assumed that $\mathbf{W}_j^{\mathrm{v}} = [\mathbf{e}_1^{N_d}, \cdots, \mathbf{e}_N^{N_d}]$ for brevity, where $\mathbf{e}_m^{N_d}, m = 1, 2, \cdots, N$ denotes the mth column of the identity matrix $\mathbf{I}_{N_d}$. Hence, we can obtain $\mathbf{H}_{ji}^{\mathrm{evv}} = \mathbf{H}_{ji}^{\mathrm{vv}} \mathbf{W}_j^{\mathrm{v}} = [\mathbf{h}_{ji1}^{\mathrm{vv}}, \cdots, \mathbf{h}_{jiN}^{\mathrm{vv}}]$, $\mathbf{H}_j^{\mathrm{ev}} = \mathbf{H}_j^{\mathrm{v}} \mathbf{W}_j^{\mathrm{v}} = [\mathbf{h}_{j1}^{\mathrm{v}}, \cdots, \mathbf{h}_{jN}^{\mathrm{v}}]$ and $(\mathbf{W}_j^{\mathrm{v}})^H \mathbf{W}_j^{\mathrm{v}} = \mathbf{I}_N$. Furthermore, $\mathbf{Z}_i^{\mathrm{v}}$ in (8) can be rewritten as $\mathbf{Z}_i^{\mathrm{v}} = \epsilon_i^{\mathrm{v}} \mathbf{I}_{N_d}$, where

$$\epsilon_i^{\mathrm{v}} = \sum_{j\in\mathcal{V}, j\neq i} \sum_{q=1}^{N} \beta_{jiq}^{\mathrm{vv}} p_{jq}^{\mathrm{v}} + \sum_{k\in\mathcal{C}} \sum_{l=1}^{N_c} \beta_{kil}^{\mathrm{cv}} p_{kl}^{\mathrm{c}}. \quad (14)$$

A. Lower Bounds on Ergodic V2V Rates

1) Maximum-Ratio Combining: For MRC detection at V2V receiver i, $\mathbf{A}_i^{\mathrm{v}} = \mathbf{H}_{ii}^{\mathrm{evv}}$ and $\mathbf{a}_{im}^{\mathrm{v}} = \mathbf{h}_{iim}^{\mathrm{evv}}$.

Proposition 1. With MRC detection at V2V receiver i and $N_d \geq 2$, the ergodic rate of V2V transmitter i R_i^{v} can be lower bounded by

$$R_{i,\mathrm{mrc}}^{\mathrm{v,lb}} = \sum_{m=1}^{N} \log_2\left(1 + \frac{p_{im}^{\mathrm{v}} \beta_{iim}^{\mathrm{vv}} (N_d - 1)}{\epsilon_i^{\mathrm{v}} + \sigma^2 + \sum_{k\neq m} p_{ik}^{\mathrm{v}} \beta_{iik}^{\mathrm{vv}}}\right). \quad (15)$$

Proof: See Appendix A. ■

Remark 1. In the denominator of (15), ϵ_i^{v} and σ^2 denote the effect of interference from other UEs and noise, respectively. The third term $\sum_{k\neq m} p_{ik}^{\mathrm{v}} \beta_{iik}^{\mathrm{vv}}$ denotes the effect of inter-stream interference. Since the length of desired V2V links are usually small, the received inter-stream interference power is usually large. Besides, the length of interfering links are usually large, and thus the received interference power from other UEs is relatively small. Intuitively, for MRC, the V2V performance is ultimately limited by inter-stream interference.

2) Zero-Forcing Receiver: For ZF detection at V2V receiver i, $(\mathbf{A}_i^{\mathrm{v}})^H \bar{\mathbf{H}}_{ii}^{\mathrm{evv}} = \mathbf{I}_N$ and $p_{im}^{\mathrm{v}} \left|(\mathbf{a}_{im}^{\mathrm{v}})^H \mathbf{h}_{iim}^{\mathrm{evv}}\right|^2 = 1$. Combining (7), (8) and (14), the SINR γ_{im}^{v} is rewritten as

$$\gamma_{im}^{\mathrm{v}} = \frac{1}{(\epsilon_i^{\mathrm{v}} + \sigma^2)(\mathbf{a}_{im}^{\mathrm{v}})^H \mathbf{a}_{im}^{\mathrm{v}}}. \quad (16)$$

Proposition 2. ZF detection is considered at V2V receiver i. With $N_d \geq N+1$, the ergodic rate of V2V transmitter i R_i^{v} is lower bounded by

$$R_{i,\mathrm{zf}}^{\mathrm{v,lb}} = \sum_{m=1}^{N} \log_2\left(1 + \frac{p_{im}^{\mathrm{v}} \beta_{iim}^{\mathrm{vv}} (N_d - N)}{\epsilon_i^{\mathrm{v}} + \sigma^2}\right). \quad (17)$$

Proof: Combining (9) and (16), we have

$$\begin{aligned} R_i^{\mathrm{v}} &\overset{(a)}{\geq} \sum_{m=1}^{N} \log_2\left(1 + \frac{1}{\mathbb{E}\left[1/\gamma_{im}^{\mathrm{v}}\right]}\right) \\ &\overset{(b)}{=} \sum_{m=1}^{N} \log_2\left(1 + \frac{1}{(\epsilon_i^{\mathrm{v}} + \sigma^2)\mathbb{E}\left[(\mathbf{a}_{im}^{\mathrm{v}})^H \mathbf{a}_{im}^{\mathrm{v}}\right]}\right) \\ &\overset{(c)}{=} \sum_{m=1}^{N} \log_2\left(1 + \frac{p_{im}^{\mathrm{v}}/(\epsilon_i^{\mathrm{v}} + \sigma^2)}{\mathbb{E}\left\{[\mathbf{B}]_{mm}\right\}}\right) \end{aligned} \quad (18)$$

where (a) follows from the convexity of the function $\log_2(1+x^{-1})$ and Jensen's inequality, (b) follows from the SINR expression in (16), $\mathbf{B} = [(\mathbf{H}_{ii}^{\mathrm{evv}})^H \mathbf{H}_{ii}^{\mathrm{evv}}]^{-1}$, $[\mathbf{B}]_{mm}$ denotes the mth row and mth column element of matrix $\mathbf{B}$, and (c) follows from $(\mathbf{a}_{im}^{\mathrm{v}})^H \mathbf{a}_{im}^{\mathrm{v}}$ = $(\mathbf{e}_m^N)^H (\mathbf{P}_i^{\mathrm{v}} (\mathbf{H}_{ii}^{\mathrm{evv}})^H \mathbf{H}_{ii}^{\mathrm{evv}})^{-1} \mathbf{e}_m^N$ = $(p_{im}^{\mathrm{v}})^{-1} [((\mathbf{H}_{ii}^{\mathrm{evv}})^H \mathbf{H}_{ii}^{\mathrm{evv}})^{-1}]_{mm}$.

By applying the identity from [10]

$$\mathbb{E}\left[\mathbf{F}^{-1}\right] = \frac{1}{N_d - N}\mathbf{I}_N \tag{19}$$

where $\mathbf{F} \sim \mathcal{W}_N^C(N_d, \mathbf{I}_N)$ is a $N \times N$ complex Wishart matrix with N_d $(N_d > N)$ degrees of freedom, we obtain

$$\mathbb{E}\left\{\left[\left((\mathbf{H}_{ii}^{\mathrm{evv}})^H \mathbf{H}_{ii}^{\mathrm{evv}}\right)^{-1}\right]_{mm}\right\} = \frac{1}{\beta_{iim}^{\mathrm{vv}}(N_d - N)}. \tag{20}$$

Plugging (20) into (18), we obtain the result in (17). ■

Remark 2. In the denominator of (17), ϵ_i^{v} and σ^2 denote the effect of interference from other UEs and noise, respectively. Proposition 2 shows that the effect of inter-stream interference vanish completely when using ZF detection. Therefore, to suppress the inter-stream interference and improve the V2V performance, we propose ZF detectors at V2V receivers.

B. Lower Bounds on Ergodic Cellular Rates

1) Maximum-Ratio Combining: For MRC detection at the BS, $\mathbf{A}^{\mathrm{c}} = \mathbf{H}^{\mathrm{c}}$ and $\mathbf{a}_{km}^{\mathrm{c}} = \mathbf{h}_{km}^{\mathrm{c}}$.

Proposition 3. Considering MRC detection at the BS and $M \geq 2$, the ergodic rate of cellular UE k R_k^{c} can be lower bounded by

$$R_{k,\mathrm{mrc}}^{\mathrm{c,lb}} = \sum_{m=1}^{N_c} \log_2\left(1 + \frac{p_{km}^{\mathrm{c}}\beta_{km}^{\mathrm{c}}(M-1)}{\epsilon_{km}^{\mathrm{c}} + \sigma^2}\right) \tag{21}$$

where

$$\epsilon_{km}^{\mathrm{c}} = \sum_{q\neq m}\beta_{kq}^{\mathrm{c}}p_{kq}^{\mathrm{c}} + \sum_{i\in\mathcal{C}, i\neq k}\sum_{q=1}^{N_c}\beta_{iq}^{\mathrm{c}}p_{iq}^{\mathrm{c}} + \sum_{j\in\mathcal{V}}\sum_{l=1}^{N}\beta_{jl}^{\mathrm{v}}p_{jl}^{\mathrm{v}} \tag{22}$$

denotes the sum of inter-stream interference and interference from other UEs.

Proof: The proof of (21) is similar to that of (15) in Prop. 1 and is omitted for brevity. ■

2) Zero-Forcing Receiver: For interference-aware ZF detection at the BS, $(\mathbf{A}^{\mathrm{c}})^H\bar{\mathbf{H}} = \mathbf{I}_B$ and $p_{km}^{\mathrm{c}}\left|(\mathbf{a}_{km}^{\mathrm{c}})^H\mathbf{h}_{km}^{\mathrm{c}}\right|^2$=1.

Proposition 4. Considering interference-aware ZF detection at the BS and $M \geq B+1$, the ergodic rate of multi-antenna cellular UE k R_k^{c} can be lower bounded by

$$R_{k,\mathrm{zf}}^{\mathrm{c,lb}} = \sum_{m=1}^{N_c}\log_2\left(1 + \frac{p_{km}^{\mathrm{c}}\beta_{km}^{\mathrm{c}}(M-B)}{\sigma^2}\right). \tag{23}$$

Proof: The proof of (23) is similar to that of (17) in Prop. 2 and is omitted due to space constraints. ■

Remark 3. For MRC, the noise power is small compared to the interference power at the BS since MRC detection can not suppress any interference. Proposition 3 shows that the cellular performance is ultimately limited by inter-stream interference, V2V-to-cellular interference and interference from other cellular UEs. Therefore, to suppress the interference and improve the cellular performance, an interference-aware ZF detector is proposed at the BS.

V. Power Control with Rate Constraints

Since V2V channels change very fast, V2V receivers report instantaneous CSI of V2V links to the BS will cause large overhead. Besides, frequent power control which is based on instantaneous CSI, will introduce large signaling overhead and a lot of processing burden. Hence, in V2V underlay cellular networks, the BS should adopt large-scale fading based power control by using the rate lower bounds.

In this section, we investigate a power control problem to maximize the sum rate of cellular UEs, while meeting the rate target of V2V UEs. To suppress the interference, we consider ZF detection at V2V receivers and interference-aware ZF detection at the BS. Moreover, the GP technique is adopted to solve the optimization power control problem.

Using the rate lower bounds, the large-scale fading based power control problem can be formulated as follows:

$$\begin{aligned}
\mathcal{P}: \quad & \underset{P_k^{\mathrm{c}}, P_i^{\mathrm{v}}}{\text{maximize}} \quad \sum_{k=1}^{K} R_{k,\mathrm{zf}}^{\mathrm{c,lb}} \\
\text{s.t.} \quad & R_{i,\mathrm{zf}}^{\mathrm{v,lb}} \geq R^{\mathrm{th}}, \ \forall i \in \mathcal{D} \\
& 0 \leq P_k^{\mathrm{c}} \leq P_{\max}^{\mathrm{c}}, \ \forall k \in \mathcal{C} \\
& 0 \leq P_i^{\mathrm{v}} \leq P_{\max}^{\mathrm{v}}, \ \forall i \in \mathcal{D}
\end{aligned}$$

where R^{th} denotes the target rate of V2V UEs, $P_{\max}^{\mathrm{c}}$ and $P_{\max}^{\mathrm{v}}$ denote the maximum transmit power of cellular UEs and V2V UEs, respectively. However, the power control problem maximizing the sum rate is difficult to get solutions. To make the problem be tractable, lower bounding of $\log_2(1+\gamma)$ by $\log_2(\gamma)$ is often used. Besides, we assume that the large-scale fading coefficients from different antennas of each UE are equal, i.e., $\beta_{km}^{\mathrm{c}} = \beta_k^{\mathrm{c}}, m = 1, \cdots, N_c$ and $\beta_{jil}^{\mathrm{vv}} = \beta_{ji}^{\mathrm{vv}}, l = 1, \cdots, N_d$. Then the power is divided equally among different streams of each UE, i.e., $p_{km}^{\mathrm{c}} = P_k^{\mathrm{c}}/N_c$ and $p_{il}^{\mathrm{v}} = P_i^{\mathrm{v}}/N$. Hence, the interference power from other UEs ϵ_i^{v} in (14) can be rewritten as

$$\epsilon_i^{\mathrm{v}} = \sum_{j\in\mathcal{V}, j\neq i}\beta_{ji}^{\mathrm{vv}}P_j^{\mathrm{v}} + \sum_{k\in\mathcal{C}}\beta_{ki}^{\mathrm{cv}}P_k^{\mathrm{c}}. \tag{24}$$

Thus, combining (17) and (23), we can approximate $\mathcal{P}$ as $\mathcal{P}_1$:

$$\begin{aligned}
\mathcal{P}_1: \quad & \underset{P_k^{\mathrm{c}}, P_i^{\mathrm{v}}}{\text{maximize}} \quad \sum_{k=1}^{K}\log_2\left(\frac{P_k^{\mathrm{c}}\beta_k^{\mathrm{c}}(M-B)}{\sigma^2 N_c}\right) \qquad (25) \\
\text{s.t.} \quad & N\log_2\left(\frac{P_i^{\mathrm{v}}\beta_{ii}^{\mathrm{vv}}(N_d-N)}{(\epsilon_i^{\mathrm{v}}+\sigma^2)N}\right) \geq R^{\mathrm{th}}, \ \forall i \in \mathcal{D} \\
& 0 \leq P_k^{\mathrm{c}} \leq P_{\max}^{\mathrm{c}}, \ \forall k \in \mathcal{C} \\
& 0 \leq P_i^{\mathrm{v}} \leq P_{\max}^{\mathrm{v}}, \ \forall i \in \mathcal{D}.
\end{aligned}$$

By introducing a new $K \times 1$ dimensional auxiliary variable $\mathbf{q}$ with its kth element $q_k \leq P_k^{\mathrm{c}}\beta_k^{\mathrm{c}}(M-B)/(\sigma^2 N_c)$, problem $\mathcal{P}_1$ can be turned into the GP problem $\mathcal{P}_2$ as follows:

$$\mathcal{P}_2: \quad \underset{P_k^{\mathrm{c}}, P_i^{\mathrm{v}}, q_k}{\text{maximize}} \quad \prod_{k=1}^{K} q_k \tag{26}$$

$$
\begin{aligned}
\text{s.t.} \quad & \frac{q_k \sigma^2 N_c}{P_k^{\mathrm{c}} \beta_k^{\mathrm{c}} (M-B)} \leq 1, \ \forall k \in \mathcal{C} \\
& \frac{(\epsilon_i^{\mathrm{v}} + \sigma^2) N}{P_i^{\mathrm{v}} \beta_{ii}^{\mathrm{vv}} (N_d - N)} 2^{\frac{R^{\mathrm{th}}}{N}} \leq 1, \ \forall i \in \mathcal{D} \\
& 0 \leq P_k^{\mathrm{c}} \leq P_{\max}^{\mathrm{c}}, \ \forall k \in \mathcal{C} \\
& 0 \leq P_i^{\mathrm{v}} \leq P_{\max}^{\mathrm{v}}, \ \forall i \in \mathcal{D}.
\end{aligned}
$$

Let $\mathbf{P}^{\mathrm{v}} = [P_1^{\mathrm{v}}, \cdots, P_D^{\mathrm{v}}]^T$, then the second constraint meeting the rate target of V2V UEs in (26) can be rewritten as

$$
\mathbf{P}^{\mathrm{v}} \geq (\mathbf{F}\mathbf{P}^{\mathrm{v}} + \mathbf{n}) 2^{\frac{R^{\mathrm{th}}}{N}} \tag{27}
$$

where $\mathbf{F} \in \mathbb{C}^{D \times D}$ is given by

$$
F_{ij} = \begin{cases} 0, & j = i \\ \frac{\beta_{ji}^{\mathrm{vv}} N}{\beta_{ii}^{\mathrm{vv}} (N_d - N)}, & j = 1, \cdots, i-1, i+1, \cdots, D \end{cases}
$$

and $\mathbf{n}$ denotes the effects of noise and cellular-to-V2V interference. As shown in [11], if the spectral radius (magnitude of maximum singular value) of $\mathbf{G} = 2^{\frac{R^{\mathrm{th}}}{N}} \mathbf{F}$ is less than 1, feasible solutions meeting the target rate R^{th} exist. Hence, R^{th} can be given as

$$
R^{\mathrm{th}} = N \log_2 \left(\rho_{\mathbf{F}}^{-1} \right) - \delta^{\mathrm{th}} \tag{28}
$$

where $\rho_{\mathbf{F}}$ is the spectral radius of $\mathbf{F}$ and $\delta^{\mathrm{th}} > 0$ is a constant. Moreover, the feasible solution of power control GP problem $\mathcal{P}_2$ in (26) also exists. Thus, by using the convex optimization toolbox in MATLAB, the optimal solution of $\mathcal{P}_2$ can be derived numerically.

VI. Numerical Results

In this section, simulation results are provided to validate the analytical results and evaluate the performance of the proposed scheme. In the simulation, we consider a circular cell, where all V2V transmitters and cellular UEs are uniformly distributed. The BS is located at the center of the cell, and the distance between each UE and the BS is no less than $R_{\mathrm{c}}/16$. For each V2V pair i, the location of V2V transmitter i is denoted by the polar coordinate $(r_i^{\mathrm{v}}, \theta_i^{\mathrm{v}})$, and the location of V2V receiver i is denoted by $(r_i^{\mathrm{v}} + L_{\mathrm{v}}, \theta_i^{\mathrm{v}})$. Here R_{c}=500 m is the cell radius, and L_{v}=50 m is the length of desired V2V links. The large-scale fading coefficient $\beta = d^{-\alpha}$, where d is the length of the link, and α=4 is the pathloss exponent of all links. We set the maximal transmit power $P_{\max}^{\mathrm{c}} = P_{\max}^{\mathrm{v}}$, resulting in an average SNR of 0 dB at the cell edge as reference. Besides, we set the constant δ^{th}=0.01.

First, we validate the accuracy of analytical lower bounds given in Section IV for different number of receive antennas. Fig. 2 shows the simulated V2V rate (sum rate of V2V UEs) and their lower bounds for MRC and ZF receivers at the optimal V2V power with K=5, D=5, N=2, M=200, and N_c=2. Fig. 3 shows the simulated cellular rate (sum rate of cellular UEs) and their lower bounds for MRC and interference-aware ZF receivers at the optimal cellular power with K=5, D=5, N_c=2, N_d=8, and N=2. As seen from Fig. 2 and Fig. 3, the lower bounds closely match their simulation results, especially for ZF and large number of receive antennas. Clearly, the ZF receiver can significantly increase the data rate compared to

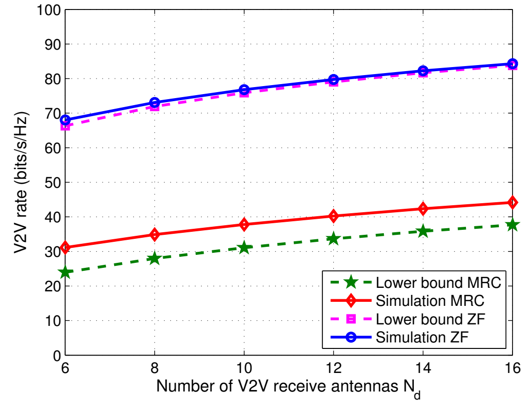

Fig. 2. V2V rate vs. number of V2V receive antennas for MRC and ZF with K=5, D=5, N=2, M=200, and N_c=2.

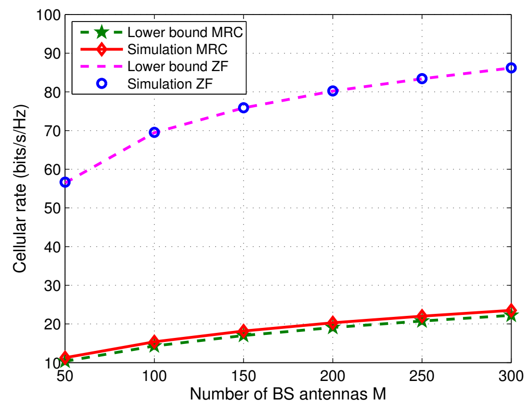

Fig. 3. Cellular rate vs. number of BS antennas for MRC and interference-aware ZF with K=5, D=5, N_c=2, N_d=8, and N=2.

the MRC receiver. Specifically, in Fig. 2, for the case with N_d=8, the simulated V2V rate of ZF is 109% higher than that of MRC. This is because ZF receivers can cancel the interference. Fig. 2 also shows that the V2V rate increases with the number of receive antennas. Thus, additional receive antennas are beneficial to improve V2V performance.

Next, more simulation results are provided. Fig. 4 shows the benefit of our proposed power control scheme over the fixed maximum power scheme. For the fixed maximum power scheme, cellular UEs and V2V transmitters transmit with maximum power and the interference is serious. In Fig. 4, we compare the cumulative distribution functions (CDFs) of per V2V UE rate, which correspond to the outage probability, for different V2V data streams with D=5, K=20, N_d=16, M=200, and N_c=1. At the same V2V UE rate, the outage probability (CDF) of our proposed scheme is smaller than that of the fixed power scheme. Moreover, the CDF curves also show that the proposed power control scheme greatly increases the V2V UE rate compared to the fixed power scheme. Specifically, at the 50 percentile, the V2V UE rate are 33% and 42% higher than that of the fixed power scheme for N=2 and N=4, respectively. Thus, our proposed scheme can provide more reliable V2V communications with higher

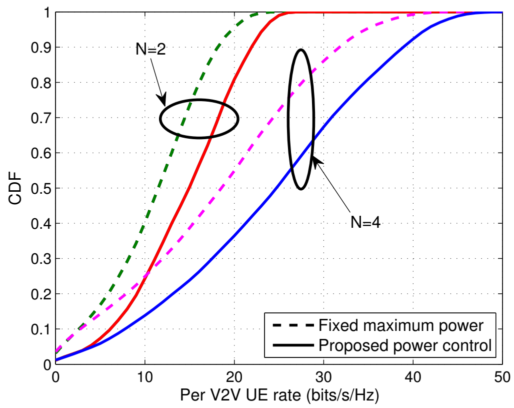

Fig. 4. CDFs of per V2V UE rate with D=5, K=20, N_d=16, M=200, and N_c=1.

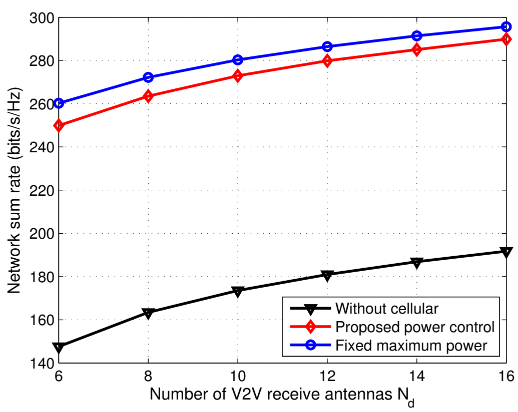

Fig. 5. Network sum rate vs. number of V2V receive antennas with D=5, N=4, K=20, M=200, and N_c=1.

data rates. It can be also seen that the V2V UE rate is higher with a larger V2V data stream, this is the benefit of spatial multiplexing gain.

Fig. 5 compares the network sum rate (sum of the cellular rate and the V2V rate) of the proposed power control scheme, the fixed maximum power scheme and the without cellular scheme with D=5, N=4, K=20, M=200, and N_c=1. For the without cellular scheme, V2V transmitters transmit with maximum power while cellular UEs keeps silent. Compared with the without cellular scheme, the proposed scheme greatly increase the network sum rate, this is the benefit of introducing cellular UEs and maximizing cellular rate. Nevertheless, the price for improving the reliability and data rates of V2V communications is visible. As shown in Fig. 5, the proposed scheme leads to a small loss of network sum rate, compared to the fixed maximum power scheme.

VII. Conclusion

In this paper, we have studied an uplink power control problem in a V2V underlay cellular network with multi-antenna UEs. Considering MRC and ZF detection, lower bounds on ergodic rates have been derived for cellular UEs and V2V UEs. Generally, ZF outperforms MRC since it can cancel interference. Using the rate lower bounds, we formulated a large-scale fading power control problem to maximize the sum rate of cellular UEs while meeting the rate constraints of V2V UEs. Further, the GP technique was adopted to solve the optimization problem. Simulation results show that our proposed power control scheme greatly increases the reliability and data rates of V2V communications compared to the fixed power scheme. The results also indicate that the proposed scheme outperforms the without cellular scheme in terms of sum rate. Moreover, the proposed power control scheme avoids reporting CSI and large overhead, compared to power control schemes based on instantaneous CSI.

Appendix A
Proof of Proposition 1

Proof: For MRC detection at V2V receiver i, $\mathbf{A}_i^{\mathrm{v}} = \mathbf{H}_{ii}^{\mathrm{evv}}$ and $\mathbf{a}_{im}^{\mathrm{v}} = \mathbf{h}_{iim}^{\mathrm{evv}}$. Combining (7), (8), (9) and (14), we have

$$R_i^{\mathrm{v}} \overset{(a)}{\geq} \sum_{m=1}^{N} \log_2\left(1+\frac{1}{\mathbb{E}\left[1/\gamma_{im}^{\mathrm{v}}\right]}\right)$$
$$\overset{(b)}{=} \sum_{m=1}^{N} \log_2\left(1+\frac{p_{im}^{\mathrm{v}}/\left(\epsilon_i^{\mathrm{v}}+\sigma^2+\sum_{k\neq m} p_{ik}^{\mathrm{v}}\beta_{iik}^{\mathrm{vv}}\right)}{\mathbb{E}\{[(\mathbf{h}_{iim}^{\mathrm{evv}})^H\mathbf{h}_{iim}^{\mathrm{evv}}]^{-1}\}}\right) \quad (29)$$

where (a) follows from the convexity of the function $\log_2(1+x^{-1})$ and Jensen's inequality, and (b) follows from (7), (8), (14) and $\mathbf{a}_{im}^{\mathrm{v}} = \mathbf{h}_{iim}^{\mathrm{evv}}$. Moreover, $(\mathbf{h}_{iim}^{\mathrm{evv}})^H\mathbf{h}_{iim}^{\mathrm{evv}} \sim \mathcal{W}_1^C(N_d, \beta_{iim}^{\mathrm{vv}})$ is a 1×1 complex Wishart matrix with N_d $(N_d>1)$ degrees of freedom [10], we get

$$\mathbb{E}\left\{\left[(\mathbf{h}_{iim}^{\mathrm{evv}})^H\mathbf{h}_{iim}^{\mathrm{evv}}\right]^{-1}\right\} = \frac{1}{\beta_{iim}^{\mathrm{vv}}(N_d-1)}. \quad (30)$$

Plugging (30) into (29), we obtain the result in (15). ■

References

[1] H. Seo *et al.*, "LTE evolution for vehicle-to-everything services," *IEEE Commun. Mag.*, vol. 54, no. 6, pp. 22–28, Jun. 2016.
[2] IMT-2020 (5G), "White paper on 5G wireless technology architecture," May 2015 [Online]. Available: http://www.imt-2020.org.cn/zh/documents/listByQuery?currentPage=1&content=
[3] G. Fodor *et al.*, "Design aspects of network assisted device-to-device communications," *IEEE Commun. Mag.*, vol. 50, no. 3, pp. 170–177, Mar. 2012.
[4] M. Botsov, M. Klugel, W. Kellerer, and P. Fertl, "Location dependent resource allocation for mobile device-to-device communications," in *Proc. IEEE WCNC*, Apr. 2014. pp. 1679–1684.
[5] W. Sun, E. G. Ström, F. Brännström, K. C. Sou and Y. Sui, "Radio resource management for D2D-based V2V communication," *IEEE Trans. Veh. Technol.*, vol. 65, no. 8, pp. 6636–6650, Aug. 2016.
[6] C.-H. Yu, O. Tirkkonen, K. Doppler, and C. Ribeiro, "Power optimization of device-to-device communication underlaying cellular communication," in *Proc. IEEE ICC*, Jun. 2009, pp. 1–5.
[7] D. Feng *et al.*, "Device-to-device communications underlaying cellular networks," *IEEE Trans. Commun.*, vol. 61, no. 8, pp. 3541–3551, Aug. 2013.
[8] D. Tse and P. Viswanath, *Fundamentals of wireless communication.* New York, USA: Cambridge University Press, 2005.
[9] B. Hassibi and B. M. Hochwald, "How much training is needed in multiple-antenna wireless links?" *IEEE Trans. Inf. Theory*, vol. 49, no. 4, pp. 951–963, Apr. 2003.
[10] D. Maiwald and D. Kraus, "Calculation of moments of complex Wishart and complex inverse Wishart distributed matrices," in *Proc. IEEE Radar, Sonar and Navig.*, 2000, pp. 162–168.
[11] R. Chen, J. G. Andrews, R. W. Heath, and A. Ghosh, "Uplink power control in multi-cell spatial multiplexing wireless systems," *IEEE Trans. Wireless Commun.*, vol. 6, no. 7, pp. 2700–2711, Jul. 2007.